KECK GEOLOGY CONSORTIUM
PROCEEDINGS OF THE TWENTY-THIRD ANNUAL KECK RESEARCH SYMPOSIUM IN GEOLOGY

ISSN# 1528-7491

April 2010

Andrew P. de Wet
Editor & Keck Director
Franklin & Marshall College

Keck Geology Consortium
Franklin & Marshall College
PO Box 3003, Lanc. Pa, 17604

Lara Heister
Symposium Convenor
ExxonMobil Corp.

Keck Geology Consortium Member Institutions:
Amherst College, Beloit College, Carleton College, Colgate University, The College of Wooster, The Colorado College Franklin & Marshall College, Macalester College, Mt Holyoke College, Oberlin College, Pomona College, Smith College, Trinity University Union College, Washington & Lee University, Wesleyan University, Whitman College, Williams College

2009-2010 PROJECTS

SE ALASKA - EXHUMATION OF THE COAST MOUNTAINS BATHOLITH DURING THE GREENHOUSE TO ICEHOUSE TRANSITION IN SOUTHEAST ALASKA: A MULTIDISCIPLINARY STUDY OF THE PALEOGENE KOOTZNAHOO FM.
Faculty: Cameron Davidson (Carleton College), Karl Wirth (Macalester College), Tim White (Penn State University)
Students: Lenny Ancuta, Jordan Epstein, Nathan Evenson, Samantha Falcon, Alexander Gonzalez, Tiffany Henderson, Conor McNally, Julia Nave, Maria Princen

COLORADO – INTERDISCIPLINARY STUDIES IN THE CRITICAL ZONE, BOULDER CREEK CATCHMENT, FRONT RANGE, COLORADO.
Faculty: David Dethier (Williams) *Students: Elizabeth Dengler, Evan Riddle, James Trotta*

WISCONSIN - THE GEOLOGY AND ECOHYDROLOGY OF SPRINGS IN THE DRIFTLESS AREA OF SOUTHWEST WISCONSIN.
Faculty: Sue Swanson (Beloit) and Maureen Muldoon (UW-Oshkosh)
Students: Hannah Doherty, Elizabeth Forbes, Ashley Krutko, Mary Liang, Ethan Mamer, Miles Reed

OREGON - SOURCE TO SINK – WEATHERING OF VOLCANIC ROCKS AND THEIR INFLUENCE ON SOIL AND WATER CHEMISTRY IN CENTRAL OREGON.
Faculty: Holli Frey (Union) and Kathryn Szramek (Drake U.)
Students: Livia Capaldi, Matthew Harward, Matthew Kissane, Ashley Melendez, Julia Schwarz, Lauren Werckenthien

MONGOLIA - PALEOZOIC PALEOENVIRONMENTAL RECONSTRUCTION OF THE GOBI-ALTAI TERRANE, MONGOLIA.
Faculty: Connie Soja (Colgate), Paul Myrow (Colorado College), Jeff Over (SUNY-Geneseo), Chuluun Minjin (Mongolian University of Science and Technology)
Students: Uyanga Bold, Bilguun Dalaibaatar, Timothy Gibson, Badral Khurelbaatar, Madelyn Mette, Sara Oser, Adam Pellegrini, Jennifer Peteya, Munkh-Od Purevtseren, Nadine Reitman, Nicholas Sullivan, Zoe Vulgaropulos

KENAI - THE GEOMORPHOLOGY AND DATING OF HOLOCENE HIGH-WATER LEVELS ON THE KENAI PENINSULA, ALASKA
Faculty: Greg Wiles (The College of Wooster), Tom Lowell, (U. Cincinnati), Ed Berg (Kenai National Wildlife Refuge, Soldotna AK)
Students: Alena Giesche, Jessa Moser, Terry Workman

SVALBARD - HOLOCENE AND MODERN CLIMATE CHANGE IN THE HIGH ARCTIC, SVALBARD, NORWAY.
Faculty: Al Werner (Mount Holyoke College), Steve Roof (Hampshire College), Mike Retelle (Bates College)
Students: Travis Brown, Chris Coleman, Franklin Dekker, Jacalyn Gorczynski, Alice Nelson, Alexander Nereson, David Vallencourt

UNALASKA - LATE CENOZOIC VOLCANISM IN THE ALEUTIAN ARC: EXAMINING THE PRE-HOLOCENE RECORD ON UNALASKA ISLAND, AK.
Faculty: Kirsten Nicolaysen (Whitman College) and Rick Hazlett (Pomona College)
Students: Adam Curry, Allison Goldberg, Lauren Idleman, Allan Lerner, Max Siegrist, Clare Tochilin

Funding Provided by: Keck Geology Consortium Member Institutions and NSF (NSF-REU: 0648782) and ExxonMobil

Keck Geology Consortium: Projects 2009-2010
Short Contributions – MONGOLIA

PALEOZOIC PALEOENVIRONMENTAL RECONSTRUCTION OF THE GOBI-ALTAI TERRANE, MONGOLIA

Project Directors: ***CONSTANCE M. SOJA*****:** Colgate University
CHULUUN MINJIN: Mongolian University of Science and Technology
Project Faculty: ***PAUL MYROW*****:** The Colorado College
D. JEFFREY OVER**:** State University of New York at Geneseo

CHEMOSTRATIGRAPHY OF THE LOWER SILURIAN SCHARCHULUUT FORMATION, YAMAAN-US, SHINE JINST REGION, GOBI-ALTAI TERRANE, MONGOLIA

UYANGA BOLD**:** Mongolian University of Science and Technology
Research Advisor: Chuluun Minjin

GEOLOGIC MAP AND PALEOECOLOGY OF THE LOWER SILURIAN SCHARCHULUUT FORMATION AT "WENLOCK HILL", SHINE JINST REGION, GOBI-ALTAI TERRANE, MONGOLIA

BILGUUN DALAIBAATAR**:** Mongolian University of Science and Technology
Research Advisor: Chuluun Minjin

SEDIMENTOLOGY, DEPOSITIONAL HISTORY AND DETRITAL ZIRCON GEOCHRONOLOGY OF THE LOWER DEVONIAN TSAKHIR FORMATION, SHINE JINST REGION, MONGOLIA

TIMOTHY M. GIBSON**:** Colorado College
Research Advisor: Paul Myrow

BRACHIOPODS FROM THE LOWER SILURIAN SCHARCHULUUT FORMATION, YAMAAN-US, SHINE JINST REGION, GOBI-ALTAI TERRANE, MONGOLIA

BADRAL KHURELBAATAR**:** Mongolian University of Science and Technology
Research Advisor: Chuluun Minjin

CHEMOSTRATIGRAPHY AND MAGNETIC STRATIGRAPHY OF THE UPPER ORDOVICIAN DARAVGAI AND GASHUUNOVOO FORMATIONS, GOBI-ALTAI TERRANE, SHINE JINST AREA, SOUTHERN MONGOLIA

MADELYN METTE: Macalester College
Research Advisor: Ray Rogers

SEQUENCE STRATIGRAPHY AND PALEONTOLOGY OF THE UPPER ORDOVICIAN DARAVGAI AND GASHUUNOVOO FORMATIONS, GOBI-ALTAI TERRANE, SHINE JINST, MONGOLIA

***SARA E. OSER*:** University of Cincinnati
Research Advisor: Carlton E. Brett

PALEOECOLOGY OF LOWER DEVONIAN (EMSIAN) SHELF DEPOSITS IN THE CHULUUN FORMATION, GOBI-ALTAI TERRANE, MONGOLIA

***ADAM FRANCIS ANTONIO PELLEGRINI*:** Colgate University
Research Advisor: Constance M. Soja

TRILOBITE PALEOECOLOGY OF THE MIDDLE DEVONIAN TSAGAANKHAALGA FORMATION NEAR TSAKHIR WELL, SHINE JINST, MONGOLIA

***JENNIFER A. PETEYA*:** Mount Union College
Research Advisor: Lee Gray

GEOLOGIC MAP SHOWING EAST-TO-WEST FACIES TRANSITIONS IN THE LOWER SILURIAN SCHARCHULUUT FORMATION, SCHARCHULUUT, SHINE JINST REGION, GOBI-ALTAI TERRANE, MONGOLIA

***MUNKH-OD PUREVTSEREN*:** Mongolian University of Science and Technology
Research Advisor: Chuluun Minjin

PALEOECOLOGY AND CHEMOSTRATIGRAPHY OF THE AMANSAIR AND TSAGAANBULAG FORMATIONS, GOBI-ALTAI TERRANE, MONGOLIA

***NADINE G. REITMAN*:** Vassar College
Research Advisor: David P. Gillikin

THE EIFELIAN GIVETIAN BOUNDARY (MIDDLE DEVONIAN) AT TSAKHIR, GOVI ALTAI REGION, SOUTHERN MONGOLIA

NICHOLAS SULLIVAN: State University of New York at Geneseo
Faculty Advisor: D. Jeffrey Over

PALEOENVIRONMENTS AND DEPOSITIONAL HISTORY OF UPPER SILURIAN-LOWER DEVONIAN LIMESTONE IN THE AMANSAIR AND TSAGAANBULAG FORMATIONS AT ULAANSHAND AND TSAKHIR, GOBI-ALTAI TERRANE, MONGOLIA

ZOE VULGAROPULOS: Oberlin College
Research Advisor: Dennis Hubbard

Funding provided by: Keck Geology Consortium Member Institutions and NSF (NSF-REU: 0648782)

Keck Geology Consortium
Franklin & Marshall College
PO Box 3003, Lancaster Pa, 17603
Keckgeology.org

PALEOECOLOGY AND CHEMOSTRATIGRAPHY OF THE AMANSAIR AND TSAGAANBULAG FORMATIONS, GOBI-ALTAI TERRANE, MONGOLIA

NADINE G. REITMAN
Vassar College
Research Advisor: David P. Gillikin

INTRODUCTION

The Gobi-Altai Terrane has been interpreted as a back-arc basin formed near the equator in the early to middle Paleozoic that was later accreted onto the Asian continent as an allochthonous terrane (Lamb and Badarch 1997; Windley et al. 2001; Badarch et al. 2002). This study aims to determine the age, paleoecology, and depositional setting of Silurian–Devonian limestone successions of the Amansair and Tsagaanbulag formations in the Ulaan Shand and Tsakhir locations of the Shine Jinst region of the Gobi-Altai. This study is the first to investigate the Silurian–Devonian boundary of the Gobi-Altai in detail and will contribute to a better understanding of the geologic history of central Asia.

METHODS

Three Silurian–Devonian sections (Fig. 1) at the Ulaan Shand and Tsakhir regions were measured, described, and photographed. The sections were selected for their preservation, exposure, and lack of deformation. The lower Tsakhir section (TSAH1) is 40 meters thick and is the oldest section in this study. The upper Tsakhir section (TSAH2) is 76 meters thick and overlies TSAH1 laterally to the east. Both Tsakhir sections are within the Tsagaanbulag Formation. The upper part of TSAH1 and the lower part of TSAH2 are strongly deformed. The TSAV section described by Vulgaropulos (this volume) is a well-preserved section of the same age as lower TSAH2, and located laterally to the west. The section at Ulaan Shand (UL2) is 33 meters thick and within the Amansair Formation, which is younger than the Tsagaanbulag Formation. The UL2 section is older than the UL1 section described by Vulgaropulos (this volume). Samples were taken from the freshest surfaces possible, at approximately one-meter intervals for petrographic analysis and half-meter intervals for isotope analysis. TSAH2 was sampled only in the top 12 meters. Stable isotope ($\delta^{13}C$ and $\delta^{18}O$) analyses were performed on a total of 100 samples from all three sections. Powdered samples were processed at the University of Arizona Environmental Isotope Laboratory and the University of Michigan Stable Isotope Laboratory. Thin sections were made from all petrographic samples (74 total). A total of 300-count point counts were performed on 18 thin sections, one every four meters through the sampled sections. X-ray diffraction (XRD) analysis was performed for all samples. Random-oriented grain mounts of isotope samples were run from 29 to 32 degrees to determine the presence and approximate percentages of dolomite. Thin sections were run from 20 to 32 degrees to determine relative intensities of quartz, calcite, and other accessory minerals.

RESULTS

Isotopes

Isotope results are variable (Fig. 1), with $\delta^{13}C$ values for TSAH1 ranging from +1.32‰ to +3.53‰, and $\delta^{18}O$ values from -14.07‰ to -10.17‰. $\delta^{13}C$ data show an increasing trend of ~1.5-2.0‰ from 18 meters to the top of the section. $\delta^{13}C$ values for TSAH2 range from -2.27‰ to -0.35‰, and $\delta^{18}O$ values range from -13.18‰ to -10.44‰. $\delta^{13}C$ values for TSAH2 range from a low of -2.21‰ near the base to -0.35‰ at 71 meters and then drop to -2.27‰ just below the Silurian–Devonian disconformity. $\delta^{13}C$ values for UL2 range from +1.36‰ to +2.91‰. The

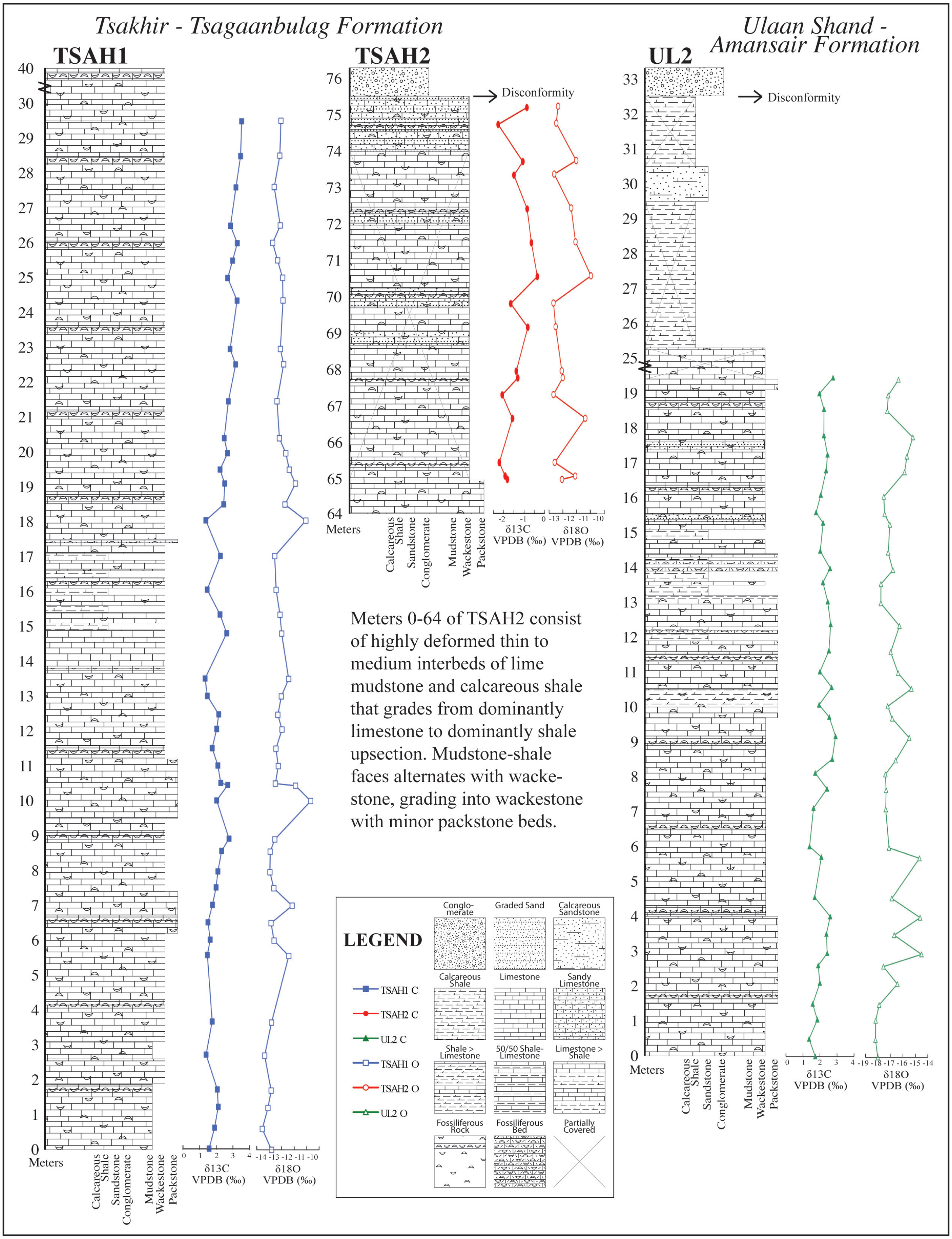

Figure 1. Stratigraphic columns reconstructed from field notes and revised according to point count data. Corresponding carbon and oxygen isotope data are shown next to the columns. The ~1.5-2.0‰ increase in $\delta^{13}C$ values near the top of TSAH1 may signify the location of the Silurian–Devonian boundary. TSAH1 is oldest, followed by TSAH2. UL2 is youngest.

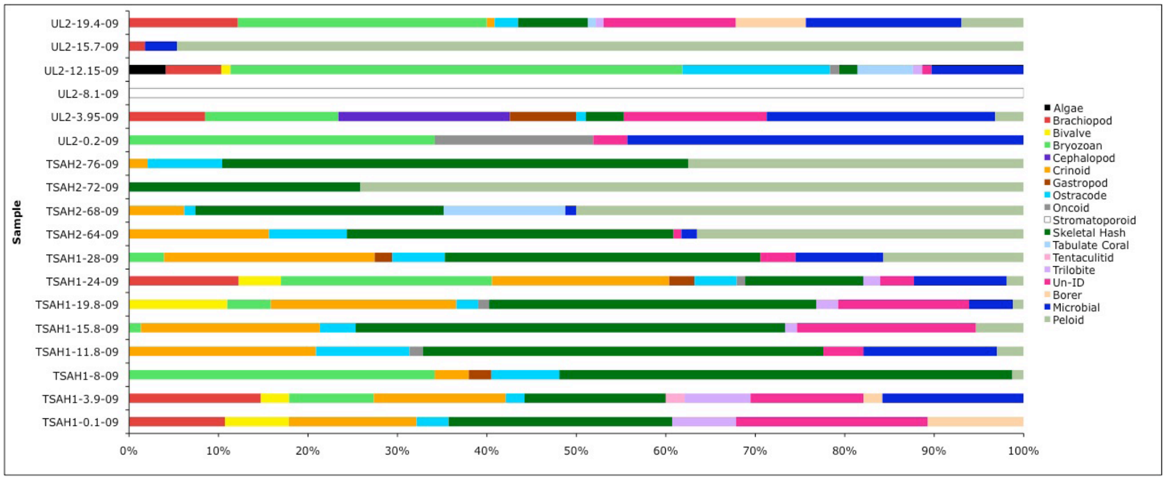

Figure 2. Fossil distribution in TSAH1, TSAH2, and UL2. Point count data from 18 samples are presented. Microbial encrustations and peloids are common in all sections. TSAH1 is characterized by abundant skeletal hash, crinoids, and ostracodes. TSAH2 is composed almost entirely of peloids, skeletal hash, crinoids, and ostracodes. UL2 displays the most biodiversity, and has abundant bryozoans and rare large (10-30 cm) stromatoporoids and cephalopods, as seen in the field as well as in thin section. Diversity of feeding strategies and diets of the recorded fossils assemblages are indications of complex marine ecosystems. Low biodiversity and abundant skeletal hash and peloids in the sampled part of TSAH2 may indicate a stressed environment.

data show long-term oscillations on the order of 1.0-1.5‰ throughout the section. $\delta^{18}O$ values for UL2 range from -14.50‰ to -18.20‰.

Lithologies

Field investigation with revision from point count data allowed the identification of distinct lithologic changes from the base of TSAH1 (oldest) to the top of UL2 (youngest) (Fig. 1).

TSAH1: This outcrop consists of blue-grey, sparse to packed bioclastic wackestone with one interval of interbedded wackestone-calcareous shale. The deposits are mostly medium to thickly bedded, with a few units of thin (5-10 cm) bedding.

LOWER TSAH2: This section consists of thin to medium interbeds of carbonate mudstone and calcareous shale that grades from dominantly limestone to dominantly shale upsection. Mudstone-shale facies alternate with blue-grey wackestone, grading up into wackestone with minor packstone beds and one bed with fine laminae and very coarse (1-2 mm) quartz grains.

UPPER TSAH2: This outcrop consists of wackestone and packstone with abundant skeletal hash. It shows a stratigraphic increase in the abundance of fine laminae, very coarse (1-2mm) quartz grains, and other siliciclastic grains. Graded bedding is present near the top below the unconformity contact with Devonian conglomerate (age from Minjin and Soja 2009).

LOWER UL2: This part of the UL2 outcrop consists of thin to medium bedded wackestone and packstone. Interbedded wackestone-calcareous shale intervals first appear stratigraphically in the middle of the section and thicken upsection. Fine laminae are more abundant upsection.

UPPER (25.5-32.5 m) UL2: This part of the outcrop consists of calcareous shale with a one-meter thick unit of more resistant calcareous sandstone below the unconformity contact with Devonian conglomerate (date from Minjin and Soja 2009).

Point Counts

The fossil assemblages of TSAH1, TSAH2, and UL2 are distinctly different from each other (Fig. 2). Encrusted skeletal fragments are common in all sections (Figs. 2, 3F). Crinoids, skeletal hash, and ostracodes are the dominant bioclasts in TSAH1. Bryozoans, trilobites, and bivalves are also present,

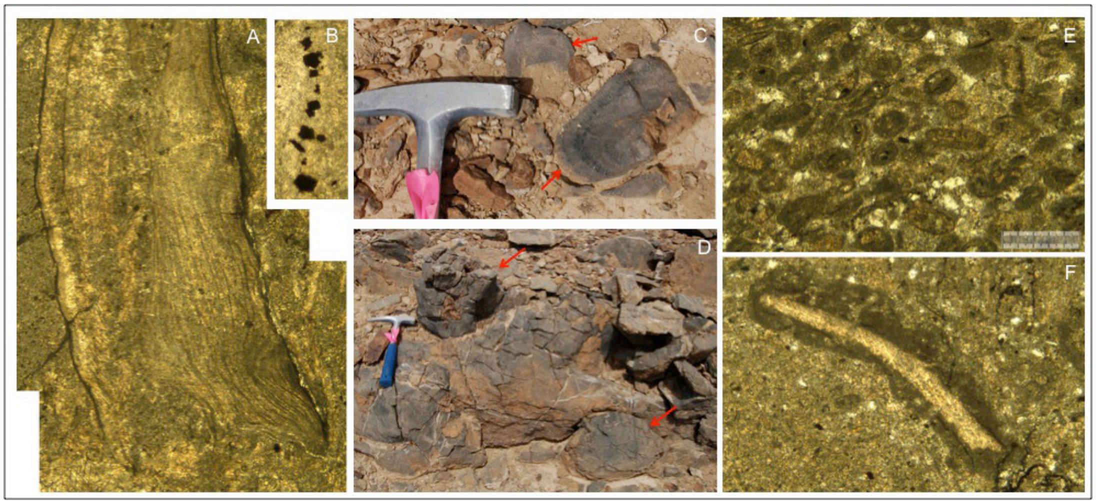

Figure 3. Common fossils and accessory minerals. A) Composite photomicrograph showing part of a thick brachiopod shell. Field of view is ~5 mm wide. Brachiopod is ~3 cm in length (full extent not seen in photo). B) Common blocky opaque minerals. Color in reflected light is brown/red, indicating hematite. Field of view is ~200 microns wide. C) Tabulate corals in calcareous shale interval just under 10.5 meters at UL2. Hammer is 28 cm long and points upsection. D) Stromatoporoids in the field just above and below 11.3 meters at UL2. E) Peloids and fossil hash common in TSAH2 and parts of UL2 seen in thin section. Scale bar is 1 mm. E) Common microbial encrustation of a skeletal fragment. Scale is the same as in E.

as well as rare oncoids and gastropods. TSAH2 is characterized by abundant skeletal hash and peloids with minor crinoids and ostracodes, but no other identifiable skeletal remains. UL2 contains abundant bryozoans and, to a lesser extent, brachiopods. UL2 shows a greater biodiversity than TSAH1 or TSAH2, with calcareous algae, trilobites, oncoids, ostracodes, and gastropods present in thin section, and few large (12 to 30 cm) tabulate corals (Fig. 3C), stromatoporoids (Fig. 3D), and cephalopods evident in the field. A large stromatoporoid (UL2-8.1-09) and a large cephalopod (UL2-3.95-09) were also detected petrographically, as well as many tabulate corals. A complete record of fossils recorded in point counts is given in Figure 2.

X-Ray Diffraction

XRD analysis of all isotope samples revealed five samples with 10-20% dolomite present. XRD data for thin sections showed more variation in mineralogy and abundant quartz and feldspar (Fig. 4). Samples are primarily calcite, with the exception of UL2-30.25, TSAH2-70.5, and TSAH2-75A, which are quartz-dominated. XRD data show abundant siliciclastic mineral input near the base of TSAH1, the top of TSAH2, and throughout UL2.

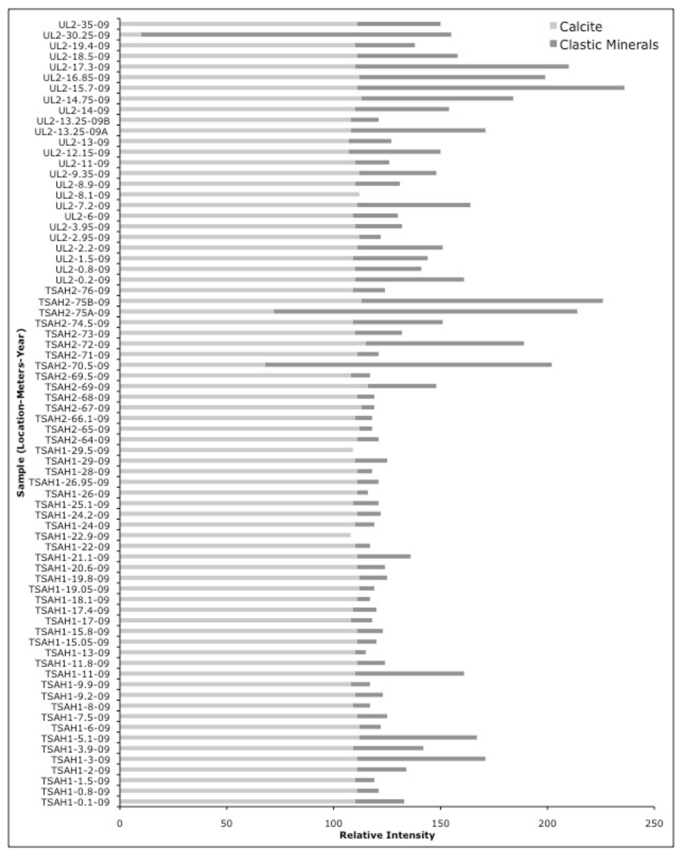

Figure 4. X-ray diffraction results from thin sections. Relative intensities of calcite and siliciclastic minerals (quartz and feldspar) show three samples dominated by siliciclastic input. High siliciclastic input indicates a shallow depositional environment.

DISCUSSION

Diagenesis

Very negative (-10.14‰ to -18.20‰) $\delta^{18}O$ values (Fig. 1) indicate possible effects from diagenesis on all samples (Brand and Veizer 1981; Sharp 2007). $\delta^{13}C$ values for TSAH1 and UL2 are standard for Silurian/Devonian marine carbonate (Brand and Veizer 1981; Saltzman 2002; Sharp 2007), but TSAH2 $\delta^{13}C$ values are more negative than expected. Taken together, $\delta^{13}C$ and $\delta^{18}O$ isotope signals imply strong alteration from post-burial diagenesis in TSAH2, but weak or no effect on TSAH1 and UL2. Cubic opaque minerals (e.g., hematite, Fig. 3B) and amorphous opaque fracture fill (pyrite and hematite) are present in many thin sections with fractures and stylolites, which also indicate diagenetic effects in all sections.

Silurian–Devonian Boundary

Previous studies have placed the Tsagaanbulag and the Amansair formations in different chronostratigraphic positions within the late Silurian to early Devonian (Wang et al. 2005; Lamb et al. 2008). The observed ~+1.5-2.0‰ trend in $\delta^{13}C$ values of TSAH1 (Fig. 1) could be preliminary evidence of the Klonk positive $\delta^{13}C$ excursion, which marks the Silurian-Devonian boundary worldwide (Brand and Veizer 1981; Saltzman 2002; Bruggisch and Mann 2004; Malkowski and Racki 2009), but more sampling of younger strata is needed to determine the precise shape of the curve. $\delta^{13}C$ values of TSAH2 and UL2 do not show evidence of an excursion and provide no further information on the location of the Silurian–Devonian boundary within the Amansair and Tsagaanbulag formations.

Depositional Environment: Fossil Evidence

The fossil assemblages observed in the field and in thin section indicate that all sections were deposited in shallow marine carbonate shelf environments. Brachiopods, cephalopods, crinoids, trilobites, and stromatoporoids usually inhabit shallow shelf zones, and oncoids commonly form in shallow shelf settings (Scholle and Ulmer-Scholle 2003). Additionally, the thick brachiopod shells evident in thin section (Fig. 3A) suggest a warm environment because brachiopod shell thickness correlates with water temperature (Scholle and Ulmer-Scholle 2003).

The observed types and distribution of fossils indicate complex marine ecosystems. The fossil assemblages provide evidence for tiering and predation, both indicators of advanced aquatic ecosystems with specialization and feeding guilds (Benton and Harper 2009). The fossil assemblage of UL2 is the most diverse, with deposit feeders (trilobites, gastropods, ostracodes), and suspension feeders (bryozoans, crinoids, corals), comprising herbivores, detritivores, and omnivores. Rare large cephalopods, a carnivorous predator, also exist at TSAH1 and UL2. Although the fossil assemblage at UL2 is more diverse, the fossil assemblages found at TSAH1 and the lower part of TSAH2 comprise organisms with the same range of feeding mechanisms and tiering levels.

The fossil assemblage observed at the top of TSAH2 shows low biodiversity, which may indicate a stressed environment. Most beds in the upper section of TSAH2 are dominated by peloids and one or two taxa (crinoids or ostracodes) of skeletal debris (Fig. 3), which may be an indication of a variable and harsh environment. Identifiable skeletal hash is composed of crinoids and ostracodes, but most skeletal hash is unidentifiable. The large percentage of crinoidal hash in TSAH2 may be misleading because echinoderms' unique petrographic characteristics make them easier to identify in thin section than other skeletal debris. Additionally, post-mortem disarticulation of crinoids creates many ossicles from one living organism. Thus, the actual relative abundance of crinoids is likely lower than represented by point counts. Low biodiversity may be due to the large proportion of unidentifiable skeletal hash, or the environment may have been too harsh (high-energy) and/or fluctuating in salinity or oxygen for other organisms to exist. Further evidence is needed to completely reconstruct the paleoecology and depositional environment of the uppermost beds of TSAH2.

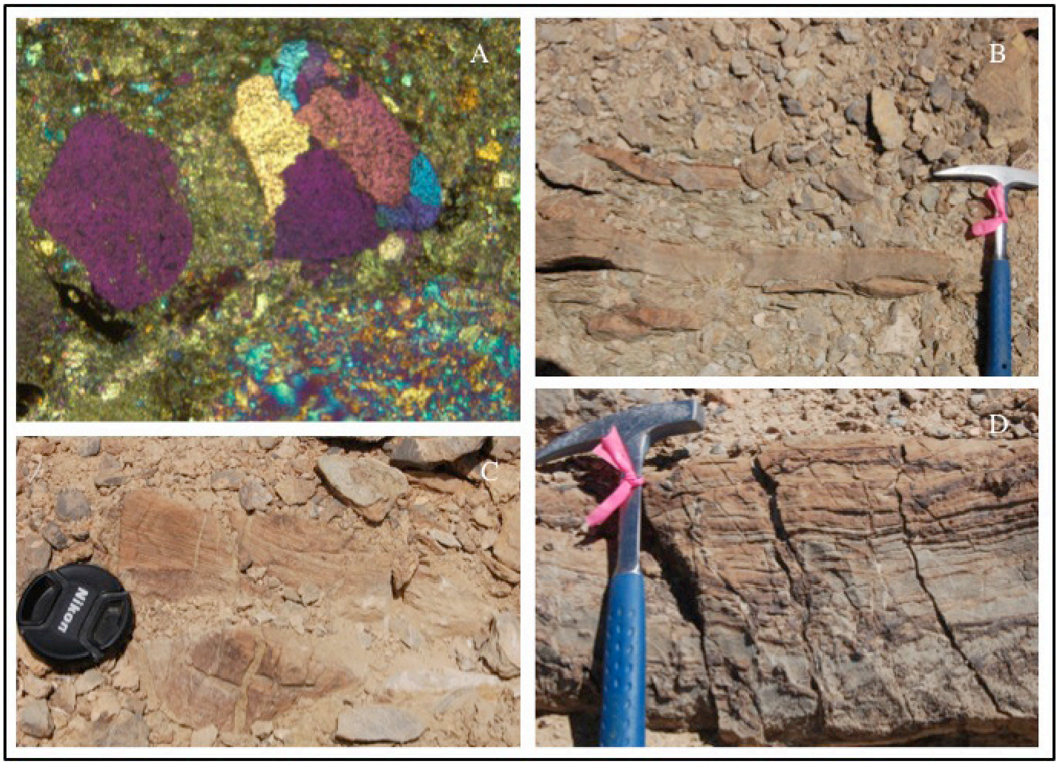

Figure 5. Evidence of shallowing at TSAH2. A) Siliciclastic grains in thin section in a sample from 70.5 meters. Clockwise from left: monocrystalline quartz, polycrystalline quartz, sandstone. Field of view is ~5 mm wide. B) Interbedded calcareous shale and limestone at 39 meters. C) Fine sandstone laminae at 58.9 meters. D) Sandstone fining upwards in the last limestone bed (75 meters) below the contact with Devonian conglomerate. Hammer is 28 cm long and points upsection.

Bryozoan, bivalve, and oncoid morphology may provide clues to the energy levels of the depositional environments. Delicate and erect bryozoans (rather than massive or encrusting ones) are indicators of low-energy environments (Scholle and Ulmer-Scholle 2003). The bryozoans at Ulaan Shand and Tsakhir are mostly large (1 to 5 cm), but grew in finger-like shapes. Neither encrusting nor massive bryozoans were found, but the bryozoans observed were not delicate. Thus, bryozoan morphology lies between delicate and massive, so energy level may also be intermediate. Bivalve shell morphology also correlates with energy level. Bivalves typically form thicker shells in high-energy environments and thinner shells in lower-energy environments (Akester and Martel 2000; Scholle and Ulmer-Scholle 2003). Bivalve shells seen in thin section are not particularly thick or thin, though sample size is small (5-10). Vedrine et al. (2007) characterize four types of oncoids based on morphology and composition of the encrusting layers, and show that each type can be attributed to a specific depositional environment. Vedrine et al. (2007) show that water energy, water depth, platform morphology, and sediment accumulation rate are all factors in oncoid formation. Oncoids found at UL2 and TSAH1 are similar to oncoids Vedrine et al. (2007) characterize as forming in moderate-energy environments in protected lagoons and high-energy environments in open lagoons (i.e., oncoids that are mm to cm in diameter; elliptical or spherical; have a visible, usually bioclastic nucleus; and have micritic laminae, sometimes encompassing other debris). Morphologies of bryozoans, bivalves, and oncoids observed in the field and in thin section from TSAH1 and UL2 indicate formation in a moderate-energy environment, with some fluctuation.

Depositional Environment: Sedimentary Evidence

The sedimentary evidence indicates that the upper part of TSAH2 was deposited in a high-energy environment. Rounded, 1-2 mm monocrystalline quartz grains and other siliciclastic grains of probable terrigenous origin, including feldspar, sandstone, and polycrystalline quartz, are found in many samples (Fig. 5A). The degree of rounding seen in thin section (Fig. 5A) may indicate a sedimentary source or long-term abrasion in a high-energy setting (Scholle and Ulmer-Scholle 2003). Additional petrographic evidence of a high-energy environment includes distinct bands of siliciclastic and skeletal debris, skeletal debris in preferred orientation (convex up), grading of skeletal debris, fine laminae (of sand/limestone) within beds (Fig. 5C), and fining upwards of siliciclastic grains within beds (Fig. 5D). There are also beds of skeletal debris in random orientation. Fossils are mostly disarticulated and crushed, with most beds dominated by unidentifiable skeletal hash. A single two-cm wide tabulate coral, though mostly whole, shows evidence of abrasion and rounding.

Evidence for a high-energy depositional environment coupled with low taxonomic diversity indicates that the top part of TSAH2 may have formed in a stressed shallow subtidal environment. Shallow subtidal deposits were affected by episodic storms and tides. TSAH2's location in the shallow subtidal zone is supported by the presence of graded beds and the inclusion of siliciclastic rock fragments within the carbonate depositional setting. An intertidal origin is unlikely given the absence of mudcracks, raindrop imprints, burrows, and ripple marks (Flugel 2004; Soja 2009).

Matrix composition and the presence of siliciclastic grains indicate that TSAH1-TSAH2 and UL2 are shallowing-upwards marine successions with fluctuations in relative sea level and depositional environments. Increasing abundance and thickness of calcareous shale intervals (Fig. 5B) in the middle of these sections, combined with an upsection increase in fine laminae and siliciclastic input (Figs. 4, 5), is evidence for a local shallowing trend, though with some relative sea level fluctuation in TSAH1 and lower-middle TSAH2. The high-energy zone at the top of TSAH2 may represent the shallowest part of the section, which was affected by marine processes such as storms and tides. UL2 contains similar calcareous shale intervals that thicken upsection. Combined with increasing abundance of fine laminae and fluctuating siliciclastic input (Fig. 4), shale intervals suggest a shallow setting with fluctuating sea level. The top seven meters of UL2 are composed of mostly-covered calcareous shale with a one-meter thick unit of resistant sandstone with calcareous cement. These upper deposits indicate that siliciclastic input was increasing enough to dominate seafloor sedimentation, but was also fluctuating. The sandstone unit within the calcareous shale interval represents a time when siliciclastic input shifted to sand (rather than clay) and increased to dominate seafloor deposition. Carbonate production slowed during this time, likely because carbonate-producing organisms were unable to adapt to increased siliciclastic input.

The local shallowing trend may be part of a larger eustatic regression spanning the Silurian–Devonian boundary or may be the result of local tectonic forces. This study finds evidence of shallowing successions in the latest Silurian to early Devonian, which are overlain by disconformal contacts with Devonian conglomerate. This evidence is supported by a similar shallowing trend at UL1 (Vulgaropulos, this volume), which is also overlain by Devonian conglomerate. Although both transgressions and regressions have been described for the Silurian–Devonian boundary interval, Malkowski and Racki (2009) report that most sea level data record a eustatic regression with a sea level drop of approximately 50 m below the shelf margin. This regression marks the decline in epicontinental seas worldwide and commonly caused erosional gaps in the rock record (Malkowski and Racki 2009). Additionally, tectonics likely affected the region in the early Devonian. The Devonian conglomerate overlying TSAH2 and UL2 has abundant cobble-size limestone clasts and few calcareous sandstone clasts, suggesting a local source for the conglomerate (Gibson, this volume). Tectonism in the Early Devonian likely uplifted the lithified sections, contributing to a fall of relative sea level.

CONCLUSION

The studied sections in the Tsagaanbulag and Amansair Formations at Tsakhir and Ulaan Shand in the Gobi-Altai Terrane likely span the Silurian–Devonian boundary and suggest a local sea level regression near the boundary. The positive increase in $\delta^{13}C$ values at the top of the TSAH1 section may represent a precursor to the upper Silurian Klonk excursion, indicating that the Silurian–Devonian boundary may be higher in the Tsagaanbulag Formation. The isotope data show minor diagenesis in two sections and possibly serious diagenesis in a third section. The studied sections were deposited in shallow, subtidal shelf environments with fluctuating siliciclastic input, varying energy levels, and complex ecosystems. The top of TSAH2 was a high-energy, possibly stressed, depositional environment affected by episodic storms. Interpretations of depositional environments indicate an overall shallowing trend, which may correspond to a local regression, either as a result of a well-known eustatic regression that spans the Silurian–Devonian boundary (Malkowski and Racki 2009), or in response to uplift in the Early Devonian that produced overlying terrestrial conglomerate.

REFERENCES

Akester, R.J., Martel, A.L. (2000) Shell shape, dysodont tooth morphology, and hinge-ligament thickness in the bay mussel Mytilus trossulus correlate with wave exposure. Canadian Journal of Zoology 78: 240-253.

Badarch, G., Cunningham, W.D., Windley, B.F. (2002) A new terrane subdivision for Mongolia: implication for the Phanerozoic crustal growth of Central Asia. Journal of Asian Earth Sciences 21: 87-110.

Benton, M. J., Harper, D.A.T. (2009) Introduction to Paleobiology and the Fossil Record. Wiley-Blackwell.

Brand, U., Veizer J. (1981) Chemical diagenesis of a multicomponent carbonate system -2: stable isotopes. Journal of Sedimentary Petrology 51(3): 987-997.

Buggisch, W., Mann, U. (2004) Carbon isotope stratigraphy of Lochkovian to Eifelian limestones from the Devonian of central and southern Europe. International Journal of Earth Sciences 93: 521-541.

Flügel, E. (2004) Microfacies of carbonate rocks: analysis, interpretation and application. Springer.

Lamb, M.A., Badarch, G. (1997) Paleozoic sedimentary basins and volcanic-arc systems of Southern Mongolia: new stratigraphic and sedimentologic constraints. International Geology Review 39: 542-576.

Lamb, M.A., Badarch, G., Navratil, T., Poier, R. (2008) Structural and geochronologic data from the Shin Jinst area, eastern Gobi Altai, Mongolia: implications for Phanerozoic intracontinental deformation in Asia. Tectonophysics 451: 312-330.

Malkowski, K., Racki, G. (2009) A global biogeochemical perturbation across the Silurian- Devonian boundary: ocean-continent-biosphere feedbacks. Palaeogeography, Palaeoclimatology, Palaeoecology 276: 244-254.

Minjin, C., Soja, C.M. (2009) Geology of the Shine Jinst area of South Mongolia. Unpublished field guidebook.

Saltzman, M.R. (2002) Carbon isotope (δ13C) stratigraphy across the Silurian-Devonian transition in North America: evidence for a perturbation of the global carbon cycle. Palaeogeography, Palaeoclimatology, Palaeoecology 187: 83-100.

Scholle, P.A., Ulmer-Scholle, D. S. (2003) A Color Guide to the Petrography of Carbonate Rocks: grains, textures, porosity, diagenesis. American Association of Petroleum Geologists Memoir

77: 2-445.

Sharp, Z. (2007) Principles of Stable Isotope Geochemistry. Pearson/Prentice Hall.

Soja, C. M. (2009) Keck/Mongolia Project Field Guidebook. Unpublished field guidebook.

Vedrine, S., Strasser, A., Hug, W. (2007) Oncoid growth and distribution controlled by sea-level fluctuations and climate (Late Oxfordian, Swiss Jura Mountains). Facies 53: 535-552.

Wang, C., Weddige, K., Chuluun, M. (2005) Age revision of some Palaeozoic strata of Mongolia based on conodonts. Journal of Asian Earth Sciences 25: 759-771.

Windley, B.F., Badarch, G., Cunningham, W.D., Kroner, A., Buchan, A.C., Tomurtogoo, O., Salnikova, E.B. (2001) Subduction-accretion history of the Central Asian Orogenic Belt: constraints from Mongolia. Gondwana Research 4: 825-826.